

# Silicon-modified Surfactants and Wetting: IV. Spreading Behaviour of Trisiloxane Surfactants on Energetically Different Solid Surfaces

R. Wagner,<sup>1\*</sup> Y. Wu,<sup>1</sup> H. v. Berlepsch<sup>1</sup> and L. Perepelittchenko<sup>2</sup>

<sup>1</sup>Max-Planck-Institute for Colloids and Surfaces, Rudower Chaussee 5, 12489 Berlin, Germany

<sup>2</sup>Institute for Petrochemical Synthesis, Leninskii Prospekt 29, 117912 Moscow, Russia

The spreading behaviour of defined trisiloxane surfactants of general formula  $[(\text{CH}_3)_3\text{SiO}]_2\text{CH}_3\text{Si}(\text{CH}_2)_3(\text{OCH}_2\text{CH}_2)_n\text{OCH}_3$  ( $n = 3\text{--}9$ ) on five different solid surfaces has been investigated. Maximum spreading areas and rates are found on non-polar or slightly polar surfaces of 30 to 40 mNm<sup>-1</sup> surface energy. Extremely low or high surface energies substantially reduce the spreading rates. On non-polar surfaces rapid spreading is observed for 1 wt % solutions of the relatively short-chained penta- and hexa-ethylene glycol derivatives. On slightly polar surfaces dilute 0.1 wt % solutions of longer-chained derivatives spread faster. This spreading pattern shift coincides with a change of the phase behaviour. Solutions of Silwet L77 do not prefer one specific surface, since 1 wt % solutions abruptly stop spreading after a few seconds and the maximum spreading rates are found for 0.1 wt % solutions. Therefore, Silwet L77 essentially belongs among the long-chained derivatives. Copyright © 2000 John Wiley & Sons, Ltd.

**Keywords:** surfactants; siloxanes; spreading; surfaces

Received 6 October 1998; accepted 19 September 1999

## 1 INTRODUCTION

Aqueous solutions of some commercially available trisiloxane surfactants (e.g. Silwet L77, in which a

polydisperse triethylene- to dodecaethylene-glycol hydrophile is attached to the trisiloxane moiety via a short trimethylene spacer) rapidly wet low-energy surfaces (water contact angle  $>90^\circ$ ).<sup>1</sup> The spreading rate of such a so-called ‘superspreader’ solution significantly exceeds that expected for a purely liquid-diffusion-controlled process.<sup>2–4</sup>

Recently, a study on 1,1,1,3,5,5,5-heptamethyl-trisiloxane and solutions of Silwet L77 showed that for the surfactant solution the radius  $r$  is proportional to time  $t^{0.65}$  whereas for the pure siloxane the relationship  $r \propto t^{0.25}$  was found. Ellipsometric investigations of the Silwet L77 solution drop edges under dynamic conditions suggest the existence of a precursor film 0.3 nm thick.<sup>5</sup>

Fast adsorption of surfactant molecules onto the substrate produces a surface tension gradient which generates a rapid surfactant molecule flow (Marangoni flow) directed towards the drop edge.<sup>6–8</sup>

However, the role of neither the surface energy/surface chemistry nor the surfactant solutions’ phase behaviour has been understood in detail.

Silwet L77 spreads on hydrophobic as well as on hydrophilic surfaces ( $0 \geq \cos\theta_{\text{water}} \geq 0.9$ ). A maximum was found for  $\cos\theta_{\text{water}} = 0.4$ ,<sup>6</sup> although the total surface energies ( $\gamma_{\text{sv}}$ ), or their Lifshitz–van der Waals ( $\gamma_{\text{sv}}^{\text{LW}}$ ) or donor–acceptor components ( $\gamma_{\text{sv}}^{+/-}$ ) have not been determined.<sup>9</sup> Further, chemically different surfaces of comparable surface energies have not been investigated.

The importance of the turbidity of trisiloxane surfactant solutions for spreading on low-energy surfaces has repeatedly been stressed.<sup>6,10</sup> This turbid two-phase state is usually adjusted by variation of the temperature<sup>11–15</sup> or the average oligoethylene glycol chain length.<sup>16</sup>

However, experiments have demonstrated that the spreading behaviour of the polydisperse Silwet L77 is nearly independent of the temperature and the phase state of the solution.<sup>6</sup> Instead, it could be

\* Correspondence to: R. Wagner, Max-Planck-Institute for Colloids and Surfaces, Rudower Chaussee 5, 12489 Berlin, Germany.  
Contract/grant sponsor: Deutsche Forschungsgemeinschaft; Contract/grant number: WA 1043/1–2.

**Table 1** Colours and purities of the siloxanyl-modified oligoethylene glycols, and their contamination compositions

Compd.	Colour	Purity (% GC)	Contamination	
			Si (%)	Without Si (%)
EO3	Colourless	≥99		
EO4	Colourless	≥99		
EO5	Colourless	99		1.0
EO6	Pale yellow	97.5	1 (EO5 type)	1.5
EO7	Pale yellow	96	1.5 (EO6 type)	2.5
EO8	Yellow	95	1.5 (EO6 type)	3.5
EO9	Pale brown (Pt)	90	10 (EO7 + EO8 type)	

shown that certain additives generate non-turbid solutions and simultaneously increase the spreading rate.<sup>17</sup> Furthermore, the spreading rates of aqueous solutions of defined oligoethylene glycol-modified hydrocarbon surfactants ( $C_iE_j$ ) do not correlate with their known microstructures.<sup>10</sup> Recent papers focus on the general ability of certain trisiloxane-based surfactants to form vesicles as an essential prerequisite for superspreading or the formation of a separate phase of accumulated surfactant molecules at the solid–liquid interface.<sup>18,19</sup>

These contrary findings clearly demonstrate that a comprehensive understanding of the superspreading phenomenon has not been reached.<sup>20</sup> A better understanding of the basic principles necessitates the investigation of sufficiently pure trisiloxane-based single compounds. Aqueous solutions of defined amino-modified trisiloxane structures rapidly spread on polypropylene. Minor changes in the amino moiety structure caused considerable differences in the spreading area.<sup>21</sup> Recently<sup>22</sup> we described the synthesis of single components of Silwet L77 bearing three to nine oligoethylene glycol units attached to the trisiloxane block. A pronounced temperature and therefore phase-type dependence of the spreading rate on non-polar, low-energy surfaces exists.<sup>23</sup> For dispersed (two-phase,  $2\Phi$ ) systems close to the transition temperature ( $T_c$ ) from the lamellar phase ( $L_\alpha$ ) to the two-phase state ( $2\Phi$ ) the highest initial spreading rates can be expected. Defined binary mixtures mimic the spreading behaviour of the equivalent single compounds with corresponding chain lengths. However, the chain length difference between the two compounds decisively influences the spreading rates.<sup>24</sup> All of these spreading experiments on single compounds and their defined mixtures have been carried out on a single non-polar, low-energy surface. The influences of surface energy and surface polarity are unknown. Therefore the

purpose of this study was to investigate the dependence of the spreading areas and the initial spreading rates of defined trisiloxane surfactants on the surface energy and surface polarity.

## 2 MATERIALS AND METHODS

### 2.1 Materials

Silwet L77 was supplied from Union Carbide. The synthesis of defined 1,1,1,3,5,5,5-heptamethyltrisiloxanyl (MD\*M) derivatives of the general structure  $[(CH_3)_3SiO]_2CH_3Si(CH_2)_3(OCH_2CH_2)_nOCH_3$  ( $n = 3–9$ ) has been outlined in an earlier paper.<sup>22</sup> Table 1 summarizes the colours, purities and product compositions of the siloxanyl-modified oligoethylene glycols.<sup>19</sup>

For the spreading experiments five chemically and energetically different silicon wafer surfaces were prepared.

Before the surface modifications the wafers were washed in ethanol, methylene chloride and diethyl ether, placed in an oxidizing solution consisting of 39 parts (w/w) of conc.  $H_2SO_4$ , 11 parts (w/w) of  $H_2O$  and 2 parts w/w of  $K_2S_2O_8$ , then rinsed with twice distilled water and finally dried in an argon stream.

In order to prepare trimethylsilylated (ME) surfaces, bare wafers were put in hexamethyldisilazane in a vacuum-tight desiccator. Surface structures of the types  $(C_2H_5)_3SiO-(ET)$ ,  $(C_6H_5)(CH_3)_2SiO-(PH)$ ,  $(C_6H_5)_3SiO-(TP)$  and  $[CH_3O(CH_2CH_2O)_5CH_2CH_2CH_2](CH_3)_2SiO-$  (EO) have been prepared from the corresponding chlorosilanes in anhydrous *n*-heptane. The chemical structures and reaction conditions are summarized in Fig. 1 and Table 2.

$[(CH_3)_3Si]_2NH$ ,  $(C_2H_5)_3SiCl$ ,  $(C_6H_5)(CH_3)_2SiCl$

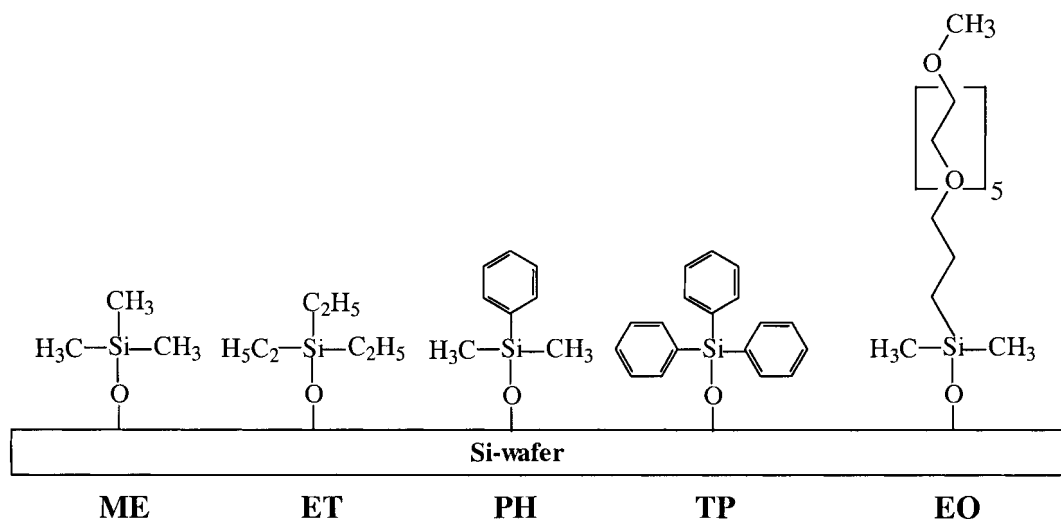


Figure 1 Surface structures of the modified silicon wafers.

and  $(\text{C}_6\text{H}_5)_3\text{SiCl}$  were commercially available (ABCR) and were used without further purification.

The silane  $[\text{CH}_3\text{O}(\text{CH}_2\text{CH}_2\text{O})_5\text{CH}_2\text{CH}_2\text{CH}_2](\text{CH}_3)_2\text{SiCl}$  was synthesized from  $\text{CH}_3\text{O}(\text{CH}_2\text{CH}_2\text{O})_5\text{CH}_2\text{CH}=\text{CH}_2$  and  $\text{H}(\text{CH}_3)_2\text{SiCl}$ . Thus, 8.3 g ( $2.84 \times 10^{-2}$  mol) of pentaethylene glycol monoallyl monomethyl ether<sup>21</sup> was stirred at 70 °C for 30 min. Volatile substances were removed in oil vacuum. Afterwards the pentaethylene glycol derivative was cooled to room temperature, then 4 g ( $4.23 \times 10^{-2}$  mol) dimethylchlorosilane and 10 mg of a 3 wt% Pt-containing Lamoreaux catalyst solution<sup>24</sup> were added under an argon atmosphere. The hydrosilylation was carried out at 70 °C for 3 h. The complete conversion of the olefin was checked by means of gas chromatography. The excess of dimethylchlorosilane was removed in oil vacuum. Without further purification 7 g of the slightly yellow oily product was injected into a vessel containing the wafer pieces and 200 ml dry n-

heptane. The temperature was raised to 70 °C for 18 h. The modified wafers were removed from the vessel and cleaned with acetone, ethanol and twice-distilled water.

The energy state of the wafers was characterized by contact-angle measurements against water and organic liquids. The energy data sets of the test liquids are given in Table 3.

Test liquid drops were placed on every piece of silicon wafer and the contact angles were determined goniometrically. The angles in Table 4 represent the mean values of at least four measurements. Deviations larger than  $\pm 1^\circ$  for single measurements were not observed.

The data for the strictly non-polar alkanes tetradecane, pentadecane, hexadecane and *cis*-decahydronaphthalene ( $\gamma_{\text{lv}} = \gamma_{\text{lv}}^{\text{LW}}$ ) as well as  $\text{CH}_2\text{I}_2$  ( $\gamma_{\text{lv}} \approx \gamma_{\text{lv}}^{\text{LW}}$ ) were used to calculate solid surface tensions  $\gamma_{\text{sv}}$  (Neumann;<sup>27</sup> Eqn [1]) and the corresponding Lifshitz–van der Waals contribution

Table 2 Modified silicon wafer surfaces: surface structures, reagents and reaction conditions

Surface structure	Reagent	Reaction time (h)	Temperature (°C)
$(\text{CH}_3)_3\text{SiO}-$	$[(\text{CH}_3)_3\text{Si}]_2\text{NH}$	144	20
$(\text{C}_2\text{H}_5)_3\text{SiO}-$	5 g $(\text{C}_2\text{H}_5)_3\text{SiCl}$ in 200 ml n-heptane	24	65
$(\text{C}_6\text{H}_5)(\text{CH}_3)_2\text{SiO}-$	5 g $(\text{C}_6\text{H}_5)(\text{CH}_3)_2\text{SiCl}$ in 200 ml n-heptane	36	65
$(\text{C}_6\text{H}_5)_3\text{SiO}-$	10 g $(\text{C}_6\text{H}_5)_3\text{SiCl}$ in 200 ml n-heptane	48	70
$[\text{CH}_3\text{O}(\text{CH}_2\text{CH}_2\text{O})_5-$	7 g $[\text{CH}_3\text{O}(\text{CH}_2\text{CH}_2\text{O})_5-$	18	70
$\text{OCH}_2\text{CH}_2\text{CH}_2](\text{CH}_3)_2\text{SiO}-$	$\text{CH}_2\text{O})_5\text{OCH}_2\text{CH}_2\text{CH}_2](\text{CH}_3)_2\text{SiCl}$ in 200 ml n-heptane		

**Table 3** Interfacial liquid/vapour tensions ( $\gamma_{lv}$ ), and Lifshitz–van der Waals ( $\gamma_{lv}^{LW}$ ) and donor–acceptor ( $\gamma_{LV}^{+/-}$ ) contributions of water and selected organic liquids

Liquid	$\gamma_{lv}$ (mN m <sup>-1</sup> )	$\gamma_{lv}^{LW}$ (mN m <sup>-1</sup> )	$\gamma_{LV}^{+/-}$ (mN m <sup>-1</sup> )
Water <sup>a</sup>	72.8	21.8	51.0
Tetradecane	26.6	26.6	0
Pentadecane	27.3	27.3	0
Hexadecane	27.6	27.6	0
<i>cis</i> -Decahydronaphthalene	31.8	31.8	0
Diiodomethane <sup>a</sup>	50.8	50.8	≈0
Ethylene glycol <sup>a</sup>	48.0	29.0	19.0
Glycerol <sup>a</sup>	64.0	34.0	30.0
Formamide <sup>a</sup>	58.0	39.0	19.0

<sup>a</sup> data taken from Ref. 25.

$\gamma_{sv}^{LW}$  (Good;<sup>28</sup> Eqn [2]). Similarity between  $\gamma_{sv}$  and  $\gamma_{sv}^{LW}$  indicates the non-polar character of a surface.<sup>21,29</sup> (Table 5)

For polar surfaces ( $\gamma_{sv} \neq \gamma_{sv}^{LW}$ ) eqn [3] has been used to calculate the donor–acceptor contribution of the solid surface tension  $\gamma_{sv}^{+/-}$  from the contact angles of the polar liquids glycerol, ethylene glycol and formamide<sup>30</sup> Fowkes' concept of interfacial tension components<sup>31</sup> has been applied to calculate  $\gamma_{sv}^{tot}$  from the single contributions (Eqn [4]).

$$\cos(\theta) = \frac{(0.015\gamma_{sv} - 2)\sqrt{\gamma_{sv}^* \gamma_{lv}} + \gamma_{lv}}{\gamma_{lv}(0.015\sqrt{\gamma_{sv}^* \gamma_{lv}} - 1)} \quad (1)$$

$$1 + \cos \theta = 2\sqrt{\frac{\gamma_{sv}^{LW}}{\gamma_{lv}^{LW}}} \quad (2)$$

$$\gamma_{lv}(1 + \cos \theta) = 2\sqrt{\gamma_{sv}^{LW} \cdot \gamma_{lv}^{LW}} + 2\sqrt{\gamma_{sv}^{+/-} \cdot \gamma_{lv}^{+/-}} \quad (3)$$

$$\gamma_{sv}^{tot} = \gamma_{sv}^{LW} + \gamma_{sv}^{+/-} \quad (4)$$

## 2.2 Methods

Column GC experiments were carried out on a Perkin–Elmer Auto System gas chromatograph. A 1 m steel column (1/8-inch; 3.2 mm) packed with Chromosorb W-AW-DCMS (80–100-mesh) and modified with 3% SE30 was used (temperature programme: 50–300 °C, heating rate 10 °C min<sup>-1</sup>; 20 min at 300 °C; FID).

Contact angles were measured with a MP 320 goniometer (20-fold magnification, Carl Zeiss Jena).

The general procedure for the spreading experiments has been described in earlier papers.<sup>22–24</sup>

The spreading experiments on the surfaces of the different silicon wafers were carried out in a laboratory kept at 21 ± 0.5 °C and 49 ± 2% relative humidity. Chemicals and equipment were stored under these conditions for at least 12 h. The wafers were cleaned carefully with twice-distilled water, ethanol then finally twice-distilled water. Before every new experiment they were exposed to atmospheric conditions for 5 min. The mixtures were

**Table 4** Contact angles (deg) of water and organic liquids on the modified silicon wafer surfaces

Liquid	ME	ET	PH	TP	EO
Water	93	90	79	59	46
Tetradecane	31				
Pentadecane	34				
Hexadecane	39				
<i>cis</i> -Decahydronaphthalene		19			
Di-iodomethane			40	37	25
Ethylene glycol			59	45	42
Glycerol			72	55	55
Formamide					39

For structures and abbreviations of modified silicon wafers, see Fig. 1.

**Table 5** Modified silicon wafer surfaces: solid surface tensions ( $\gamma_{sv}$ ), Lifshitz–van der Waals ( $\gamma_{sv}^{LW}$ ) and donor–acceptor ( $\gamma_{sv}^{+/-}$ ) contributions

	ME	ET	PH	TP	EO
$\gamma_{sv}(\text{mN m}^{-1})$ (Neumann)	23	30	41	42	47
$\gamma_{sv}^{LW}(\text{mN m}^{-1})$ (Good)	23	30	39	41	46
$\gamma_{sv}^{+/-}(\text{mN m}^{-1})$	0	0	1	3	4
$\gamma_{sv}^{tot}(\text{mN m}^{-1})$	23	30	40	44	50

For structures and abbreviations, see Fig. 1.

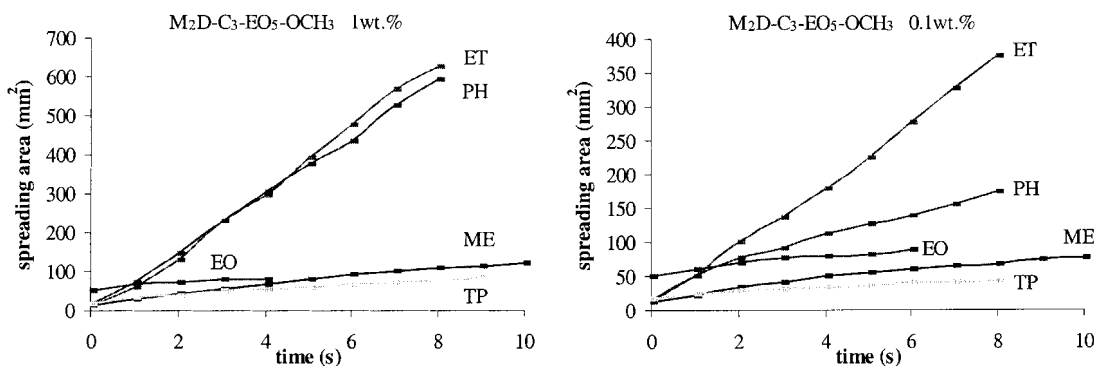
shaken manually for 2 min and afterwards ultrasonicated for 2 min in a water bath. A microsyringe was used to deposit 10- $\mu\text{l}$  drops of the surfactant solutions on the modified silicon wafers.

Each spreading experiment was repeated twice with identically pretreated wafers. The spreading drops were recorded with a standard VHS-C camcorder (25 frames  $\text{s}^{-1}$ ). The single runs were visualized on a conventional TV screen and the drop sizes determined manually. Depending on the spreading rate, up to 1 frame  $\text{s}^{-1}$  was evaluated. The setting of the starting points (spreading time = 0) was critical. Drops (10  $\mu\text{l}$ ) of a 1 wt% solution of the triethylene glycol derivative EO3 did not spread; they covered equilibrium areas of 12.5 mm<sup>2</sup> (ME), 12.5 mm<sup>2</sup> (ET), 14.9 mm<sup>2</sup> (PH), 17.5 mm<sup>2</sup> (TP) and 50.2 mm<sup>2</sup> (EO), respectively. It is important to note that a 10  $\mu\text{l}$  drop of twice-distilled water occupied 20 mm<sup>2</sup> on the EO surface. However, even minor amounts of all trisiloxane surfactants (0.001 wt%) enlarged the area to typically 50 mm<sup>2</sup>. These areas defined the starting points of the spreading experiments. The mean spreading areas were calculated

as the average from the single-run data for a given time. Typically, the deviation of single-run results from the mean values was less than 10%.

The macroscopic drop shapes frequently deviated from circles, but we did not find any rule governing this deviation. The effect disappeared after additional cleaning procedures. Minor amounts of surface impurities probably caused the irregular drop shapes.

The samples for the phase investigations were prepared by mixing the surfactants with twice-distilled water in glass test-tubes. After mixing, the solutions were subjected to a heating and cooling cycle to solubilize and homogenize the mixtures. The phase transition temperatures were determined after equilibration by visual inspection of the solutions in a thermostated water bath between crossed polarizers. The temperature at which the mixtures change from transparent to turbid can be determined in this way with an accuracy of  $\pm 0.1^\circ\text{C}$ . Birefringence indicates the presence of anisotropic liquid-crystalline phases. Flow birefringence was observed upon stirring.

**Figure 2** Time-dependent spreading areas for the derivative EO5:  $c = 1$  wt% (left);  $c = 0.1$  wt% (right).

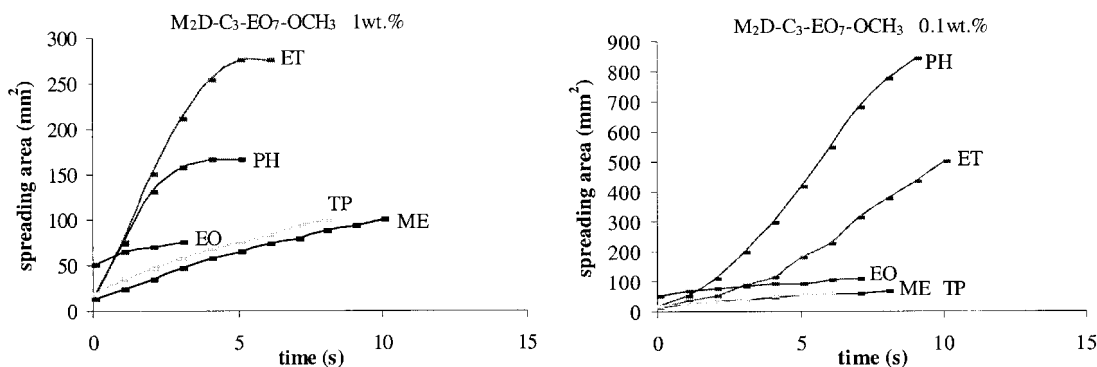


Figure 3 Time-dependent spreading areas for the derivative EO7:  $c = 1$  wt% (left);  $c = 0.1$  wt% (right).

### 3 RESULTS

Figures 2–4 describe the time dependence of the spreading areas for 1 wt% and 0.1 wt% solutions of the single compounds EO5 and EO7 as well as Silwet L77.

Slowly spreading drops were observed for up to 45 s. Generally, they reached spreading areas of less than  $200 \text{ mm}^2$  without any pronounced spreading features. Rapidly spreading drops often reached the wafer edges after less than 10 s. However, the characteristic aspects such as high initial spreading rates or sudden stops were observed reliably within this narrow time window. We therefore limited the time scales in Figs 2–4 to 15 s.

The fastest area increase for the short-chained derivative EO5 was found for the 1 wt% solution on the ET surface. EO7 spreads rapidly on the PH surface at a concentration of 0.1 wt%. Silwet L77

spreads most rapidly on both the ET and PH surfaces at a concentration of 0.1 wt%.

Figures 5–11 depict the concentration and surface energy dependence of the initial spreading rates for the derivatives EO4–EO9 and Silwet L77. EO4 is a poor spreader. EO5 and EO6 reach the spreading rate maximum on the ET surface. The longer chained derivatives EO7 and EO8 spread faster on the PH surface. Silwet L77 spreads fastest on both the ET and PH surfaces. Substantially reduced initial spreading rates were found on the extremely low-energy ME as well as on the high-energy TP and EO surfaces.

The initial spreading rates of Silwet L77 on different substrates are compared in Fig 12. On thiol-modified gold layers<sup>6</sup> a broader range of surface energies is acceptable.

Figure 13 summarizes the phase transition temperatures of the single compounds at a con-

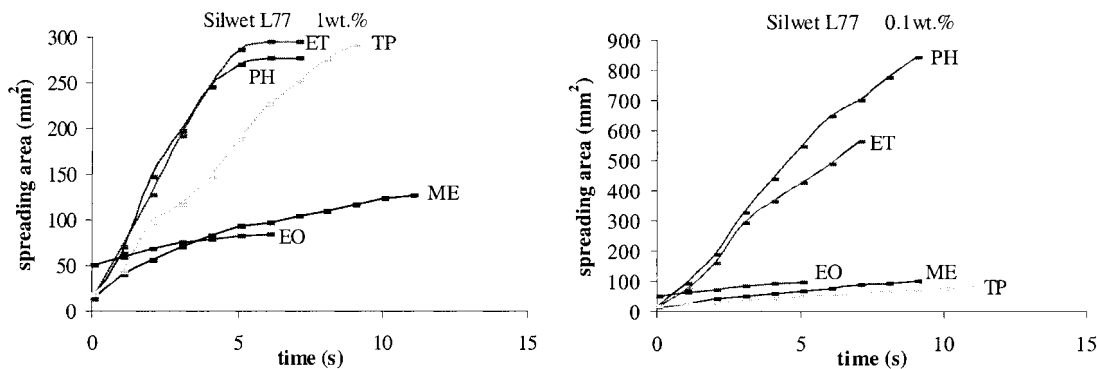
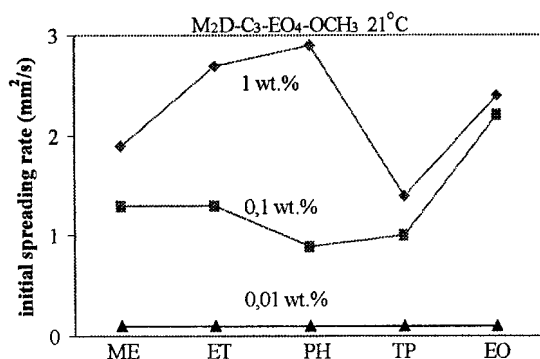
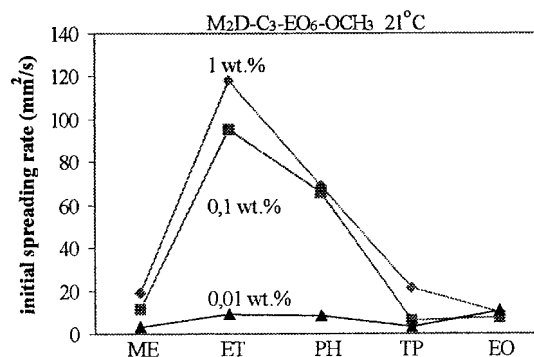


Figure 4 Time-dependent spreading areas for Silwet L77:  $c = 1$  wt% (left);  $c = 0.1$  wt% (right).



**Figure 5** EO4: concentration and surface energy dependence of the initial spreading rates.



**Figure 7** EO6: concentration and surface energy dependence of the initial spreading rates.

centration of 1 wt%. The general pattern of the phase behaviour of the single compounds has already been outlined<sup>23,24</sup> and agrees qualitatively with that for the commercially available polydisperse trisiloxane superspreaders.<sup>12,13,16</sup>

Single surfactant solutions were more or less turbid at low temperatures and showed birefringence. On increasing the temperature the solutions became increasingly transparent and showed the typical texture of a lamellar phase between crossed polarizers. We assume by analogy with related hydrocarbon<sup>14</sup> and siloxane-based compounds<sup>12,13,16</sup> that the mixtures were dilute dispersions of bilayer aggregates ( $L_\alpha$  phase). Upon an increase of temperature the samples became cloudy but isotropic and showed complete phase separation after some hours. This two-phase state is designated  $2\Phi$  and the liquid–liquid insolubility boundary is specified as the cloud point  $T_c$ . An intermediate

flow birefringent sponge phase ( $L_3$  phase) could not be identified reliably for 1 wt% solutions.<sup>23,24</sup>

## 4 DISCUSSION

### 4.1 Contact angles and surface energies

The different surfaces (Table 2) were prepared to imitate qualitatively some commonly used materials such PDMS (ME), polyethylene and polypropylene (ET), polystyrene (PH) and polyethylene glycol (EO). The major advantage of wafers is the smoothness of their surfaces. The data in Tables 4 and 5 show that the evaluation of the hydrophobic character of a surface exclusively by water contact angle measurements is insufficient. For the tri-

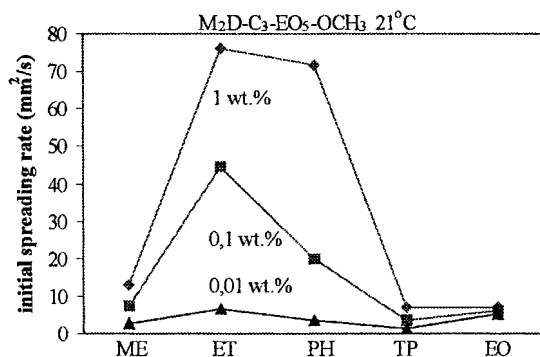


**Figure 6** EO5: concentration and surface energy dependence of the initial spreading rates.

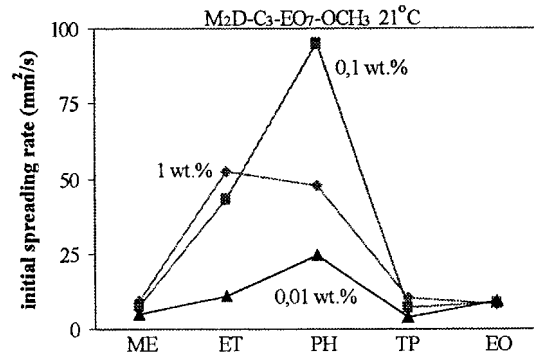


**Figure 8** EO7: concentration and surface energy dependence of the initial spreading rates.

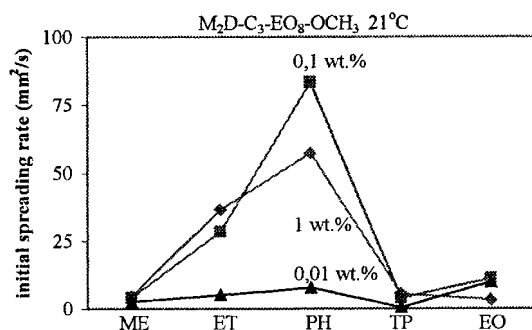


**Figure 9** EO8: concentration and surface energy dependence of the initial spreading rates.

methylsilylated (ME) and triethylsilylated (ET) surfaces the water contact angle difference amounts to a marginal  $3^\circ$ . However, the surface energy of both non-polar surfaces, calculated from contact angles of organic liquids, differs by a considerable  $7 \text{ mN m}^{-1}$ . These apparently contradictory results are due to a fundamental difference between polar organic liquids and water. The energy balance for water is dominated essentially by donor–acceptor forces, whereas for alkanes and even for organic liquids as polar as glycerol the Lifshitz–van der Waals contribution dominates (Table 3).<sup>9,26</sup> The latter force pattern better matches that of the surfaces under investigation, and causes a more sensitive reaction of the contact angles of organic liquids to differences in surface chemistry.

## 4.2 Initial spreading rate of single compounds and surface energy

It has been shown<sup>6</sup> that the initial spreading rates of

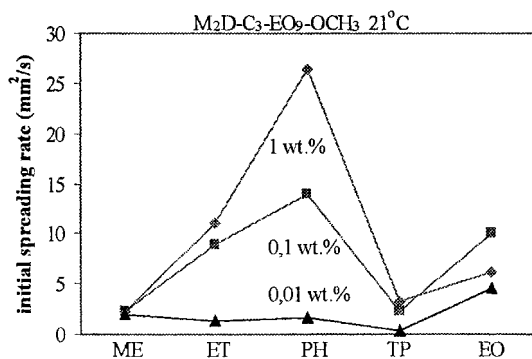


**Figure 10** EO9: concentration and surface energy dependence of the initial spreading rates.

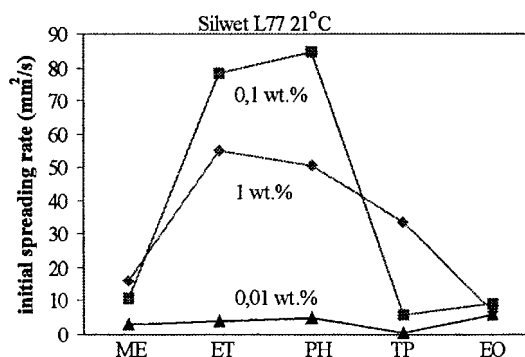


**Figure 11** Silwet L77: concentration and surface energy dependence of the initial spreading rates.

Silwet L77 and related polydisperse trisiloxane surfactants depend strongly on the surfactant concentration and the hydrophilic/hydrophobic character of the surface. A maximum in the range 0.1–0.2 wt% exists for moderately hydrophobic surfaces. Due to the surface preparation process (adsorption of thiol mixtures onto gold surfaces), neither the exact surface structures nor surface energies have been determined. Further, the spreading temperature plays no major role.

Due to an extensive study of the temperature dependence of the initial spreading rate,<sup>22–24</sup> the rapid spreading of aqueous solutions of single oligoethylene-glycol-modified trisiloxane surfactants on a non-polar, low-energy surface (trimethylsilylated Si wafer;  $\gamma_{sv} = 24 \text{ mN m}^{-1}$ ) is linked to the existence of a microdispersed two-phase state ( $2\Phi$ ). Rapid spreading is strongly temperature-dependent and occurs if the lamellar phase ( $L_\alpha$ )  $\rightarrow$

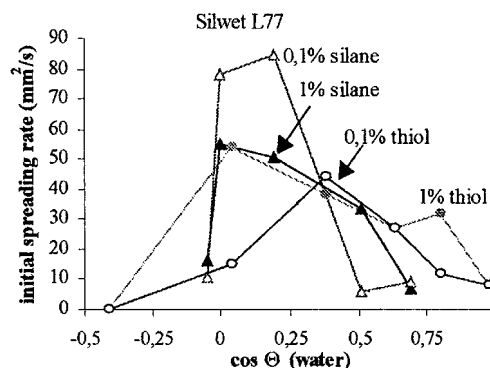


**Figure 12** Silwet L77: surface energy dependence of the initial spreading rates on silane-modified Si wafers (see Fig. 10) and thiol-modified gold layers (data taken from Ref. 6).



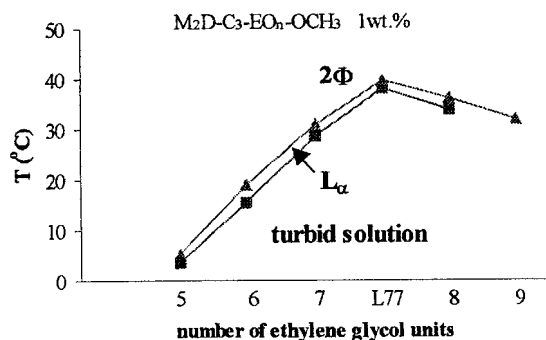


**Figure 13** Phase transition temperatures as a function of the oligoethylene glycol chain length;  $c = 1$  wt.%.

two phase state ( $2\Phi$ ) individual phase transition temperature ( $T_c$ ) is slightly below the actual spreading temperature. Within a concentration range of 0.01–1 wt% initial spreading rates increase monotonically with concentration.

This apparently contradictory behaviour highlights the necessity for an investigation of the spreading behaviour of single compounds and defined mixtures on, well-characterized smooth surfaces.

Derivative EO4 is a very poor spreader (Fig. 5). The spreading rate differences for the surfaces are not significant. For the derivatives EO5–EO9 (Figs 5–10), pronounced surface energy and concentration dependences of the initial spreading rate exist.

The data for the trimethylsilylated surface ME ( $\gamma_{sv} = 23 \text{ mN m}^{-1}$ ) are unexpected. In earlier experiments<sup>24</sup> we measured initial spreading rates of up to  $60 \text{ mm}^2 \text{ s}^{-1}$  (EO6 at  $23^\circ\text{C}$ ) on a non-polar, slightly less hydrophobic trimethylsilylated surface ( $\gamma_{sv} = 24 \text{ mN m}^{-1}$ ). The apparently marginal reduction of  $\gamma_{sv}$  is responsible for dramatically decreased initial spreading rates. Even for the best single spreader, EO6, they do not exceed  $20 \text{ mm}^2 \text{ s}^{-1}$ . We assume that below  $\gamma_{sv} = 23 \text{ mN m}^{-1}$  trisiloxane-based surfactant solutions lose the ability to wet solid materials rapidly. However, the well-established spreading rate sequence  $\text{EO6} > \text{EO5} \approx \text{EO7} > \text{EO8} > \text{EO9} > \text{EO4}$  is not altered and the initial spreading rates increase monotonically with concentration.<sup>24</sup>

A comparison of these trends with those for the ET surface ( $\gamma_{sv} = 30 \text{ mN m}^{-1}$ ) indicates an exclusively quantitative nature of the considerable spreading rate differences. On the ET surface (i) EO6 remains the fastest spreader, (ii) the derivatives' spreading rate sequence holds and (iii) the spreading rate increases with concentration. There-

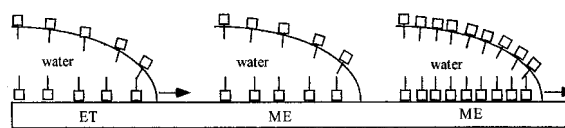


**Figure 14** Spreading of surfactant solutions on ME and ET surfaces.

fore, an optimized (fast) spreading process of a single compound on the ET surface is also linked to the existence of a microdispersed two-phase state ( $2\Phi$ ).<sup>23,24</sup>

It is assumed that the higher spreading rates on the ET surface are due to less strict demands for the coverage of the interfaces (Fig. 14, left). Recently, for a siloxane surfactant–non-polar solid surface, system the liquid/vapour ( $\gamma_{LV}$ ) and solid/liquid ( $\gamma_{SL}$ ) interfacial tensions were determined under identical dynamic conditions.<sup>32</sup> The data indicate that  $\gamma_{SL}$  reacts sensitively under dynamic conditions whereas  $\gamma_{LV}$  remains almost unaffected. Siloxane surfactant molecules probably cover a liquid–vapour interface much faster than a hydrophobic solid–liquid one. Therefore the spreading condition  $\Theta = 0^\circ$  should depend mainly on sufficient coverage of the solid–liquid interface.<sup>19</sup> It is clear that the necessarily dense coverage of the ME surface (Fig. 14, right) consumes more time and therefore limits the spreading rate.

It is one of the most interesting features of this investigation on single compounds that the spreading pattern changes qualitatively from the strictly non-polar ET to the slightly polar PH surface. A detailed inspection of the spreading rates offers some unexpected trends. It has already been reported that on the ET surface the short-chained derivatives EO5 and EO6 (Figs 6 and 7) are the fastest spreaders, and spreading rates generally increase with concentration. However, on the PH surface the 0.1 wt% solutions of the longer-chained derivatives EO7 and EO8 (Figs 8 and 9) spread faster than the corresponding EO5 and EO6 solutions and reach the highest absolute initial spreading rates. It follows immediately that for a given hydrophobic moiety the choice of an optimized oligoethylene glycol chain does not depend exclusively on  $T_c$ . Surface energy and possibly surface chemistry play a major role.

The analysis of the area vs time curves somewhat improves our understanding of the underlying processes. For derivative EO5 (Fig. 2) the spreading areas increase constantly during a relatively long time interval. Neither the surfactant concen-

tration nor the nature of the surface alters this general pattern. Whereas the 0.1 wt% solution of derivative EO7 follows this rule, its 1 wt% solution behaves differently; the spreading process stops abruptly after a few seconds on the ET and PH surfaces (Fig. 3).

An explanation of this complex behaviour requires a consideration of the fact that this general change of the spreading pattern coincides with that of the phase behaviour (Fig. 13). Solutions of EO5 ( $T_c$  5.3 °C) and EO6 ( $T_c$  19.1 °C) represent dispersed two-phase ( $2\Phi$ ) systems at a spreading temperature of 21 °C. Solutions of the longer-chained derivatives EO7 ( $T_c$  31 °C) and EO8 ( $T_c$  36 °C) undergo the phase transition lamellar phase ( $L_\alpha$ )  $\rightarrow$  two-phase state ( $2\Phi$ ) at temperatures above the spreading temperature. Under experimental conditions they remain in a vesicular/lamellar one-phase state. It is reasonable to assume that due to the inevitable water evaporation their 1 wt% solutions rapidly form highly viscous, surfactant-rich vesicular/lamellar phases at the drop edge.<sup>16,18</sup> Dilute 0.1 wt% solutions are less sensitive to the water loss. For the microdispersed systems of EO5 and EO6, viscosity arguments based on the existence of specifically organized phases are not relevant.

A further increase of the surface energy and its donor–acceptor portion causes dramatically reduced initial spreading rates. However, on the completely phenylated surface TP, the pattern of the initial spreading rates is similar to that described for the PH surface. The 1 wt% solutions of the dispersed two-phase systems EO5 and EO6 (Figs 6 and 7) spread faster than the dilute ones. Conversely, the 0.1 wt% solutions of EO7 and EO8 (Figs. 8 and 9) spread slightly better than the corresponding surfactant-rich systems. Clearly, surfaces of the PH type which bear both methyl and slightly polar phenyl groups are optimized for methylated siloxane structures and their polar oxygen atoms.<sup>33</sup>

Spreading on the oligoethylene-glycol-modified surface EO proceeds differently. Within the concentration range under investigation a significant concentration dependence of the initial spreading rate was not found. All solutions, except 0.01 wt% of EO4 (Fig. 5) spread at  $2\text{--}10\text{ mm}^2\text{ s}^{-1}$ . Specific interactions between the oligoethylene glycol moieties of the surfactant molecules and those of the modified surface probably dominate.<sup>6</sup> One of the characteristic aspects of the spreading of siloxane surfactants on low-energy surfaces, the formation of a dense siloxane layer at the solid–liquid interface is not favoured energetically. An

alternative driving force for the rapid coverage of the solid–liquid interface does not exist.

It has been demonstrated that the spreading behaviour of solutions of defined trisiloxane surfactants is a function of the phase state of the solutions and the energy/chemical character of the solid surface. From a practical point of view, a comparison with solutions of Silwet L 77 is important.

As seen in Fig. 11, Silwet L77 does not prefer a particular surface. The highest spreading rates for a given solution concentration were measured on the ET and PH surfaces. The 0.1 wt% solutions spread faster than the 1 wt% systems. An analysis of the corresponding area vs time curves (Fig. 4) discloses the affinity to the longer-chained derivatives EO7 and EO8. During a long-lasting spreading process, the diluted 0.1 wt% system can cover large areas. The spreading front of the 1 wt% solution stops abruptly after a few seconds. Phenomenologically, this profile of Silwet L77 mimics that of a long-chained derivative ( $T_c > T_{\text{spreading}}$ ) containing a certain amount of a short-chained structure. Additionally, the ability to wet the completely phenylated surface TP could be addressed by the presence of minor amounts of very long-chained species (10–12 ethylene glycol units).

However, on the present level of understanding, crucial problems remain unsolved. It is a question of far-reaching practical importance whether the matching of the energy or chemical features of surfaces and surfactants is a prerequisite for rapid spreading. A comparison of the spreading rates of Silwet L77 solutions on silane-modified Si wafers with those obtained on mixed thiol surfaces (different mixtures of  $\text{CH}_2\text{OH}$ - and  $\text{CH}_3$ -terminated thiols on gold)<sup>6</sup> (Fig. 12) suggests a considerable influence of the surface chemistry. Generally, for thiol-modified surfaces spreading is possible on a much broader range of surface energies (expressed in terms of water contact angles). On the silane-modified wafers a shift of the surface energy is linked to a change in the silane substituent structure. A substantially narrower range of accepted surfaces is found. Systematic spreading experiments on surfaces of identical surface energy but different surface chemistry could provide conclusive evidence for the dominance of either energy or chemical factors.

Further, it is not well understood why dispersed two-phase systems spread faster and over large areas on non-polar, low-energy surfaces whereas vesicular/lamellar solutions prefer moderately polar and higher-energy ones. The considerations

outlined above, concerning different surfactant densities on non-polar surfaces or the change in the surfactant orientation on polar surfaces, do not explain the mode of action of this bulk property.

### 4.3 Conclusion

The spreading behaviour of solutions of single trisiloxane surfactants on solid materials depends sensitively on the surface energy and surface chemistry. Maximum spreading areas and rates are found on non-polar (ET) or slightly polar (PH) surfaces of medium surface energy ( $30\text{--}40\text{mNm}^{-1}$ ).

For the optimized surfaces ET and PH, spreading behaviour and phase behaviour are closely related. On the non-polar surface ET, rapid spreading is observed for 1 wt% solutions of relatively short-chained derivatives (EO5 and EO6). On the slightly polar surface PH, dilute 0.1 wt% solutions of longer-chained derivatives (EO7 and EO8) spread faster. This change of the spreading pattern coincides with that of the phase behaviour. At 21 °C spreading temperature, solutions of EO5 and EO6 represent dispersed two-phase systems ( $2\phi$ ) whereas EO7 and EO8 form vesicular/lamellar systems.

Extremely low (ME) or high surface energies (PH, EO) substantially reduce the spreading rates. Nevertheless, the spreading pattern on the ME surface is qualitatively similar to that on the ET one. On the other hand, no correlation between surfactant structure, concentration and spreading behaviour was found on the EO surface. The mechanisms promoting the spreading process on low- and medium-energy surfaces are not relevant any longer.

Solutions of Silwet L77 have no preference for a specific surface. They spread fast on the ET and PH surfaces. Since 1 wt% solutions abruptly stop spreading after few seconds and the maximum spreading rates are found for 0.1 wt% solutions, Silwet L77 essentially belongs to the long-chained derivatives. However, in order to evaluate the relative influences of long- and short-chained derivatives, an investigation of less complex mixtures is necessary.

Trisiloxane surfactants have been investigated: their major disadvantage is their hydrolytic instability.<sup>34</sup> Alternatively, hydrolytically stable trimethylsilane-based materials have been developed.<sup>35</sup> The properties of this surfactant type will be reported in a separate paper.

**Acknowledgements** The project 'Polyhydroxylated silicon compounds' is supported by the Deutsche Forschungsgemeinschaft (Reg. no. WA 1043/1–2).

### REFERENCES

1. Zhu S, Miller WG, Scriven LE, Davis HT. *Colloids Surfaces* 1994; **90**:63.
2. Tiberg F, Cazabat AM. *Europhys. Lett.*, 1994; **25**:205.
3. Tiberg F, Cazabat AM. *Langmuir* 1994; **10**:2301.
4. De Connick J, Frayssé N, Valignat MP, Cazabat AM. *Langmuir* 1993; **9**:1906.
5. Pfohl T. Ph.D. thesis, University Potsdam, 1998, p. 104–105.
6. Stoebe T, Lin Z, Hill RM, Ward MD, Davis HT. *Langmuir* 1996; **12**:337.
7. Stoebe T, Lin Z, Hill RM, Ward MD, Davis HT. *Langmuir* 1997; **13**:282.
8. Svitova T, Hoffmann H, Hill RM. *Langmuir*, 1996; **12**:1712.
9. Good RJ. *J. Adhes. Sci. Technol.* 1992; **6**:1269.
10. Stoebe T, Lin Z, Hill RM, Ward MD, Davis HT. *Langmuir* 1997; **13**:7270.
11. Stürmer A, Thunig C, Hoffmann H, Grüning B. *Tenside Surf. Det.* 1994; **31**:90.
12. Hill RM, He M, Davis HT, Scriven LE. *Langmuir* 1994; **10**:1724.
13. He M, Hill RM, Lin Z, Scriven LE, Davis HT. *J. Phys. Chem.* 1993; **97**:8820.
14. Strey R, Schomacker R, Roux D, Nallet F, Olson U. *J. Chem. Soc., Faraday Trans.* 1990; **86**:2253.
15. Pandya KP, Lad KN, Bahadur P. *Tenside Surf. Det.* 1996; **33**:374.
16. Kunieda H, Taoka H, Iwanaga T, Harashima A. *Langmuir* 1998; **14**:5113.
17. Rosen MJ, Song LD. *Langmuir* 1996; **12**:4945.
18. Venzmer J, Wilkowski SP. Trisiloxane Surfactants—Mechanisms of Spreading and Wetting. In *Pesticide Formulations and Application Systems*, Vol 18, ASTM STP 1347 Nalewaja JD, Gross GR, Scott RS, (eds). Am. Soc. for Testing and Materials: Philadelphia, 1998.
19. Svitova T, Hill RM, Smirnova Y, Stuermer A, Yakubov G. *Langmuir* 1998; **14**:5023.
20. Hill RM. *Curr. Opin. Coll. Interf. Sci.* 1998; **3**:247.
21. Wagner R, Richter L, Weißmüller J, Reinert J, Klein K-D, Schaefer D, Stadtmüller S. *Appl. Organomet. Chem.* 1997; **11**:617.
22. Wagner R, Wu Y, Czichocki G, v. Berlepsch H, Weiland B, Rexin F, Perepelitchenko L. *Appl. Organomet. Chem.* 1999; **13**:611–620.
23. Wagner R, Wu Y, Czichocki G, v. Berlepsch H, Rexin F, Perepelitchenko, L. *Appl. Organomet. Chem.* 1999; **13**: 201–208.
24. Wagner R, Wu Y, Czichocki G, v. Berlepsch H, Rexin F, Rexin T, Perepelitchenko L. *Appl. Organomet. Chem.* 1999; **13**: 621–630.
25. Lamoreaux HF, US Patent 3220972, 1965.
26. Good RJ, van Oss CJ. The Modern Theory of Contact

- Angles and the Hydrogen Bond Components of Surface Energies. In *Modern Approaches to Wettability: Theory and Application*, Schrader ME, Leob G, (eds). Plenum Press: New York, 1991; 1–27.
27. Driediger O, Neumann AW, Sell PJ. *Kolloid-Zeitschr. Z. Polym.* 1965; **204**:101.
28. van Oss CJ, Chaudhury MJ, Good RJ. *Chem. Rev.* 1988; **88**:927.
29. Wagner R, Richter L, Wu Y, Weißmüller J, Reiners J, Hengge E, Kleewein A, Hassler K. *Appl. Organomet. Chem.* 1997; **11**:645.
30. Owens DK, Wendt RC. *J. Appl. Polym. Sci.* 1969; **13**:1741.
31. Fowkes FM. *Ind. Eng. Chem.* 1964; **56**:40.
32. Wagner R, Wu Y, Richter L, Siegel S, Weißmüller J, Reiners J. *Appl. Organomet. Chem.* 1998; **12**:843.
33. Wagner R, Richter L, Wu Y, Weißmüller J, Kleewein A, Hengge E. *Appl. Organomet. Chem.* 1998; **12**:265.
34. Knoche M, Tamura H, Bukovac MJ. *J. Agric. Food Chem.* 1991; **39**:202.
35. Klein KD, Knott W, Koerner G. Silicone Surfactants — Development of Hydrolytically Stable Wetting Agents. In *Organosilicon Chemistry II*, Auner N, Weis J, (eds). VCH: Weinheim, 1996; 613–618.